

## ARTICLE

# Mechanistic Investigation on the Reaction of $O^-$ with $CH_3CN$ Using Density Functional Theory

Feng Yu, Li-xia Wu, Xiao-guo Zhou\*, Shi-lin Liu

*Hefei National Laboratory for Physical Sciences at Microscale, Department of Chemical Physics, University of Science and Technology of China, Hefei 230026, China*

(Dated: Received on May 25, 2010; Accepted on June 8, 2010)

The potential energy profile of the reaction between the atomic oxygen radical anion and acetonitrile has been mapped at the G3MP2B3 level of theory. Geometries of the reactants, products, intermediate complexes, and transition states involved in this reaction have been optimized at the (U)B3LYP/6-31+G(d,p) level, and then their accurate relative energies have been improved using the G3MP2B3 method. The potential energy profile is confirmed via intrinsic reaction coordinate calculations of transition states. Four possible production channels are examined respectively, as  $H^+$  transfer, H-atom transfer,  $H_2^+$  transfer, and bimolecular nucleophilic substitution ( $S_N2$ ) reaction pathways. Based on present calculations, the  $H_2^+$  transfer reaction is major among these four channels, which agrees with previous experimental conclusions.

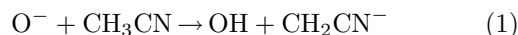
**Key words:** Atomic oxygen radical anion, Acetonitrile, Reaction mechanism, G3MP2B3, B3LYP

## I. INTRODUCTION

The reactions between atomic oxygen radical anion ( $O^-$ ) and neutral molecules have attracted much attention because of their important roles in many fields, such as ionospheric chemistry, combustion chemistry, radiation chemistry, and organic chemistry [1]. Numerous experimental studies have confirmed that many chemical active negative ions can be generated from the reactions of  $O^-$  with neutral molecules directly [1, 2]. For example, the reaction of  $O^-$  with ethylene ( $C_2H_4$ ) can produce vinylidene anion ( $CH_2=C^-$ ) [3], and halogen substituted carbene anions can be generated from the reactions of  $O^-$  with halogen substituted methane [4]. Therefore, it is necessary to investigate these reactions more extensively for ionospheric chemistry, combustion chemistry, organic chemistry, and so on. Moreover, to study these reactions will give insights into the synthesis of organic intermediate anions and exploring the mechanisms for the liquid phase chemical reactions.

Among all the anion-molecule reactions involving  $O^-$ , the reactions of  $O^-$  with substituted methane are very significant due to their potential applications in atmospheric gases detection using chemical ionization mass spectrometry (CIMS) and synthesis of the carbene anions via  $H_2^+$  transfer from substituted methane to  $O^-$  [1]. Acetonitrile ( $CH_3CN$ ) is a typical substituted methane, and there are four possible thermodynamic

production channels for reaction of  $O^-$  with  $CH_3CN$ .



As noted above, these four production channels are defined as  $H^+$  transfer (Eq.(1)), H-atom transfer (Eq.(2)),  $H_2^+$  transfer (Eq.(3)), and bimolecular nucleophilic substitution ( $S_N2$ ) reaction channels (Eq.(4)), respectively [1]. Previous experimental works [1, 5–8] showed that  $O^-$  could react with  $CH_3CN$  rapidly, but the branching ratios would vary wildly with different experimental conditions and detection techniques. Dawson and Jennings obtained the production branching ratio as  $CH_2CN^-$  (30%),  $OH^-$  (10%),  $HCCN^-$  (60%) by employing an extensively modified ion cyclotron resonance (ICR) spectrometer [5]. The reaction rate coefficient was measured to be  $3500 \mu m^3/(molecule \ s)$  by utilizing the selected ion flow tube (SIFT) apparatus operated at 297 K, and the unique anionic product  $CH_2CN^-$  was observed [6]. Grabowski and Melly reported a different branching ratio as  $CD_2CN^-$  (16%),  $OD^-$  (6%),  $DCCN^-$  (78%) when they studied the reaction of  $O^-$  with  $CD_3CN$  using the flowing afterglow (FA) apparatus operated at 300 K, and no isotope effect was observed in the branching ratio [7]. Yang *et al.* observed  $HCCN^-$  as anionic product of the  $H_2^+$  transfer pathway when they studied the reaction between hydrated  $O^-$  clusters and  $CH_3CN$  [8]. Significantly, it should be noted that secondary reactions for the title

\* Author to whom correspondence should be addressed. E-mail: xzhou@ustc.edu.cn, Tel.: +86-551-3600031

reaction would influence the determination of the product branching ratio in previous experiments [1]. Dawson and Jennings concluded that the anionic product  $\text{HCCN}^-$  would react with  $\text{CH}_3\text{CN}$  via associative detachment to produce electron and corresponding neutral molecular products [5], while Grabowski and Melly confirmed that both  $\text{OH}^-$  and  $\text{HCCN}^-$  reacted with  $\text{CH}_3\text{CN}$  via proton transfer to produce  $\text{CH}_2\text{CN}^-$  as secondary anionic product [7].

As far as we know, no quantum chemical calculation has been performed to investigate mechanism for the reaction of  $\text{O}^-$  with  $\text{CH}_3\text{CN}$ . In this work, we try to explore the mechanism for this reaction at a high G3MP2B3 [9] level of theory. The reaction processes for the aforementioned four possible production channels are examined in detail, and thus the previous experimental conclusions are also explained based on our calculations. Furthermore, the application of density functional theory (DFT) B3LYP method [10, 11] on this reaction is appraised based on current calculations.

## II. COMPUTATIONAL METHODS

All calculations are carried out with the Gaussian 03 program package [12]. A high level G3MP2B3 method [9] which has been successfully applied to study the reaction mechanisms of  $\text{O}^-$  with ethylene ( $\text{C}_2\text{H}_4$ ) [13] and vinyl radical ( $\text{C}_2\text{H}_3$ ) [14] is utilized to map the potential energy profile for the title reaction. In addition, B3LYP method [10, 11] has been proved to be suitable to characterize the stationary points on the potential energy surfaces (PESs) for the reactions of  $\text{O}^-$  with methyl fluoride ( $\text{CH}_3\text{F}$ ) [15], acetylene ( $\text{C}_2\text{H}_2$ ) [16], and benzene ( $\text{C}_6\text{H}_6$ ) [17], respectively. Moreover, it is important to involve diffuse functions and polarization functions in the basis sets to describe the anion-molecule reactive systems [18, 19]. Thus, the geometries of reactants, products, intermediate complexes (denoted as IM), and transition states (denoted as TS) of the title reaction are optimized at the (U)B3LYP/6-31+G(d,p) level of theory, and then harmonic frequencies and zero point energies (ZPEs) are calculated at the same level subsequently. The scaling factors for the harmonic frequencies [20] and ZPEs [9] are all set at 0.96. For the transition states, mass-weighted intrinsic reaction coordinate (IRC) calculations [21, 22] are performed to confirm the reaction processes. Natural bond orbital analysis (NBO) including natural population analysis (NPA) [23–27] using self-consistent-field (SCF) density with 6-31+G(d,p) basis set is employed to reveal the characteristics of various intermediate complexes on the PES. Unlike the standard auto-fashion G3MP2B3 method incorporated in Gaussian 03 program package, our modified version G3MP2B3 method is based on the molecular structures and thermochemistry analysis obtained at the (U)B3LYP/6-31+G(d,p) level, and projected UMP2 [28–30] energies are used instead of

UMP2 energies for the open-shell species to avoid spin contamination. A larger basis set aug-cc-pVTZ [31] is utilized to re-optimize the molecular structures to explore the basis set effect. Note that all numerical integrations are performed with the default (75, 302) pruned grid unless otherwise noted.

## III. RESULTS AND DISCUSSION

The optimized geometries of reactants, products, reaction intermediate complexes, and transition states on the PES are shown in Fig.1. The title reaction proceeds on the doublet state PES, and therefore it is important to check spin contamination for the current hybrid functional B3LYP calculations. As listed in Table I, the  $\langle \hat{S}^2 \rangle$  values before annihilation for all doublet molecular structures are close to 0.75. Therefore, the spin contamination is not severe and our calculations are reliable. The G3MP2B3 relative energies at 0 K of various species are summarized in Table I, and the corresponding reaction potential energy profile is shown in Fig.2. G3MP2B3 reaction enthalpies at 298.15 K for various channels are also shown in Table I, and they are consistent with the experimental data taken from Ref.[1]. As shown in Fig.1, optimized geometric parameters at (U)B3LYP/6-31+G(d,p) level are similar to the ones at (U)B3LYP/aug-cc-pVTZ level. Thus the following discussions are based on the optimized geometries at (U)B3LYP/6-31+G(d,p) level and G3MP2B3 relative energies unless otherwise noted.

In general, association process plays an important role in the initial reaction between ion and neutral molecule. Due to the long-range ion-dipole interaction,  $\text{O}^-$  associates with  $\text{CH}_3\text{CN}$  rapidly without any barrier to form an ion-dipole intermediate complex with  $C_s$  symmetry and  $^2A'$  electronic ground state, which is denoted as IM1. IM1 can also be viewed as a hydrogen-bonding complex. As shown in Fig.1, bond length of the C–H bond proximate to  $\text{O}^-$  of IM1 is larger than that of C–H bond in  $\text{CH}_3\text{CN}$ , and this elongation is due to charge transfer from the lone pair orbital of  $\text{O}^-$  to C–H antibonding  $\sigma^*$  orbital of  $\text{CH}_3\text{CN}$  from a NBO donor-acceptor standpoint [27]. The energy of IM1 is 83.6 kJ/mol below the reactants as shown in Table I, indicating a strong binding between  $\text{O}^-$  and  $\text{CH}_3\text{CN}$ . As an energized intermediate complex, IM1 can subsequently isomerize and dissociate to various final products rapidly. Note that only IM1 is located as intermediate complex on the entrance-channel PES for this reaction.

### A. $\text{H}^+$ transfer and H-atom transfer reaction channels

As shown in Fig.2, IM1 can isomerize to form IM2 via TS1, and this isomerization process is confirmed by the IRC calculation performed on TS1. Both TS1 and IM2 have  $C_s$  symmetry and the electronic states for TS1 and IM2 are both  $^2A'$ . NPA on IM2 shows

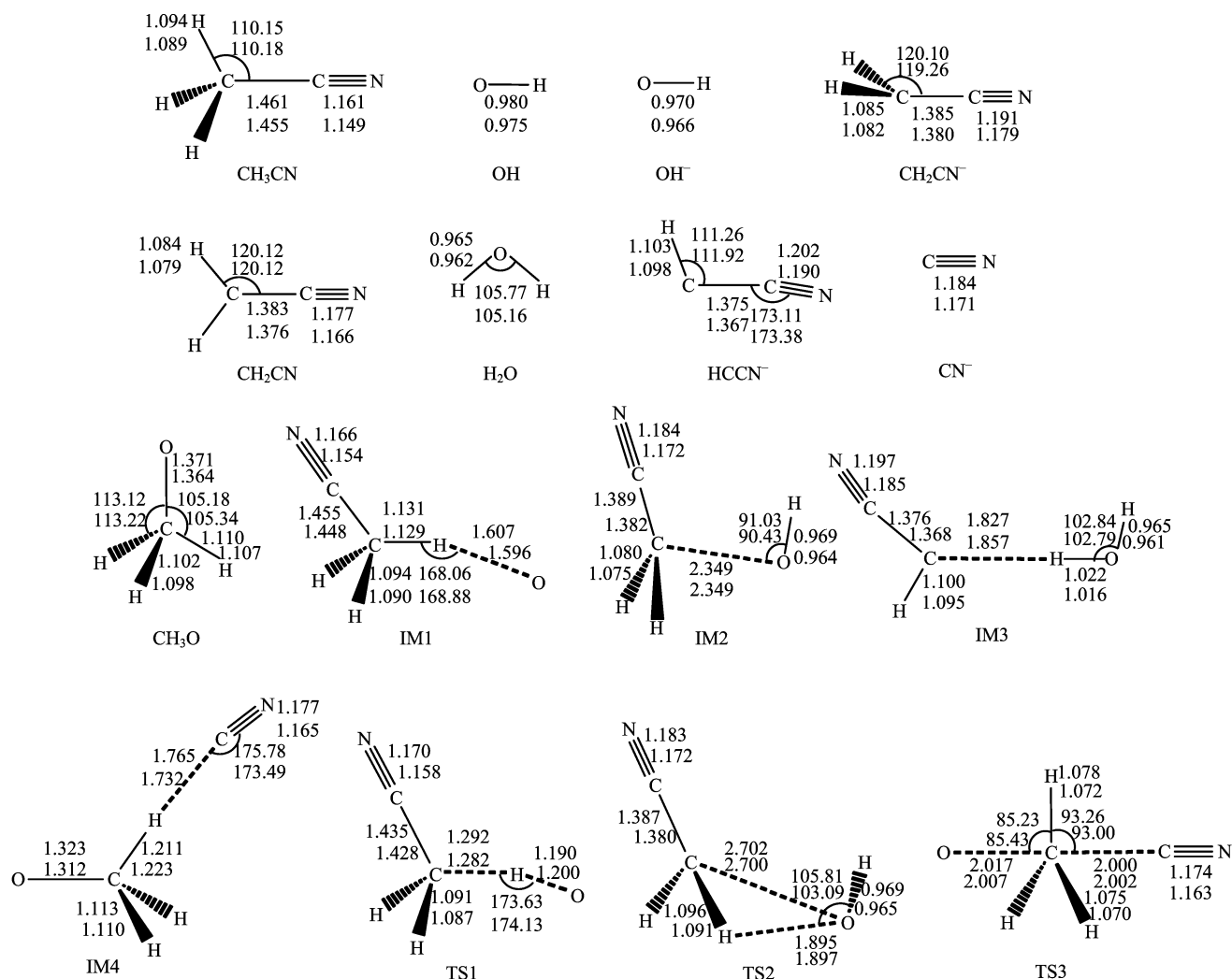


FIG. 1 Optimized geometries of the reactants, products, reaction intermediate complexes, and transition states on the PES. The upper values are the optimized geometric parameters at (U)B3LYP/6-31+G(d,p) level, and the lower are ones at (U)B3LYP/aug-cc-pVTZ level. Bond lengths are in Å and bond angles are in ( $^{\circ}$ ).

that the sum of atomic charges populated on OH group and  $\text{CH}_2\text{CN}$  group are  $-0.581$  and  $-0.419$ , respectively. Therefore, we cannot define  $\text{IM2}$  as  $\text{OH}^- \cdots \text{CH}_2\text{CN}$  or  $\text{OH} \cdots \text{CH}_2\text{CN}^-$  intermediate complex arbitrarily, and  $\text{TS1}$  cannot be defined as  $\text{H}^+$  transfer or H-atom transfer transition state either. However, it is obvious that  $\text{IM2}$  can dissociate to  $\text{OH}^- + \text{CH}_2\text{CN}$  and  $\text{OH} + \text{CH}_2\text{CN}^-$  at last via the clearance of the weak  $\text{C} \cdots \text{O}$  bond, which correspond to H-atom transfer and  $\text{H}^+$  transfer channels, respectively. Along the dissociation process initiated at  $\text{IM2}$ , if the charge transfers from  $\text{CH}_2\text{CN}$  group to OH group, the products of  $\text{OH}^- + \text{CH}_2\text{CN}$  will be formed; on the contrary, if the charge transfers from OH group to  $\text{CH}_2\text{CN}$  group, the products of  $\text{OH} + \text{CH}_2\text{CN}^-$  will be formed. Actually, according to previous calculations [32, 33], the PES of  $\text{OH} \cdots \text{CH}_2\text{CN}^-$  could be viewed as low-lying electronic excited state PES of  $\text{OH}^- \cdots \text{CH}_2\text{CN}$ , and nona-

diabatic transition between these two lower PESs responds to the  $\text{H}^+$  transfer and H-atom transfer channels. Due to the degeneracy in energy of these two PESs,  $\text{IM2}$  has characters of both  $\text{OH}^- \cdots \text{CH}_2\text{CN}$  and  $\text{OH} \cdots \text{CH}_2\text{CN}^-$ .

## B. $\text{H}_2^+$ transfer reaction channel

Besides the direct dissociation pathways mentioned above,  $\text{IM2}$  can also overcome  $\text{TS2}$  to form  $\text{IM3}$ . Forward and reverse IRC calculations confirm this reaction process. Figure 1 shows that the molecular structure of  $\text{TS2}$  with  $\text{C}_1$  symmetry is similar to  $\text{IM2}$ , so that  $\text{TS2}$  is a typical early barrier.  $\text{IM3}$  has  $\text{C}_s$  symmetry and  $^2\text{A}''$  electronic ground state. Molecular structure and natural charge distribution ( $-0.873$  on  $\text{HCCN}$  group while  $-0.127$  on  $\text{H}_2\text{O}$  group) imply that  $\text{IM3}$  is indeed an ion-dipole intermediate complex formed by  $\text{H}_2\text{O}$  and

TABLE I Imaginary frequencies of the transition states on the PES,  $\langle \hat{S}^2 \rangle$  before annihilation of all open-shell species, relative energies of all species at 0 K, and reaction enthalpies at 298.15 K for all production channels.

Species	Imaginary frequencies <sup>a</sup> /cm <sup>-1</sup>	$\langle \hat{S}^2 \rangle$ <sup>b</sup>	Relative energies <sup>c</sup> /(kJ/mol)	Reaction enthalpies/(kJ/mol)	
				This work(G3MP2B3)	Ref.[1]
O <sup>-</sup> +CH <sub>3</sub> CN		0.7548	0.0	0.0	
OH+CH <sub>2</sub> CN <sup>-</sup>		0.7524	-53.5	-50.0	-39.0
OH <sup>-</sup> +CH <sub>2</sub> CN		0.7681	-70.0	-67.5	-73.2
H <sub>2</sub> O+HCCN <sup>-</sup>		0.7648	-153.1	-149.9	-146.0
CN <sup>-</sup> +CH <sub>3</sub> O		0.7535	-111.2	-110.2	-93.7
IM1		0.7554	-83.6		
IM2		0.7591	-184.8		
IM3		0.7648	-214.6		
IM4		0.7557	-153.1		
TS1	780i <sup>d</sup>	0.7588	-71.2		
TS2	206i	0.7626	-161.8		
TS3	582i	0.7572	33.9		

<sup>a</sup> Calculated at (U)B3LYP/6-31+G(d, p) level and the scaling factor is 0.96 [20].

<sup>b</sup> For open-shell molecular structures optimized at (U)B3LYP/6-31+G(d,p) level.

<sup>c</sup> Calculated using our modified version of G3MP2B3 method.

<sup>d</sup> Imaginary frequency without scaling of TS1 is 813i cm<sup>-1</sup> at (U)B3LYP/6-31+G(d,p) level and 904i cm<sup>-1</sup> at (U)B3LYP/aug-cc-pVTZ level, which is obviously affected by the basis sets.

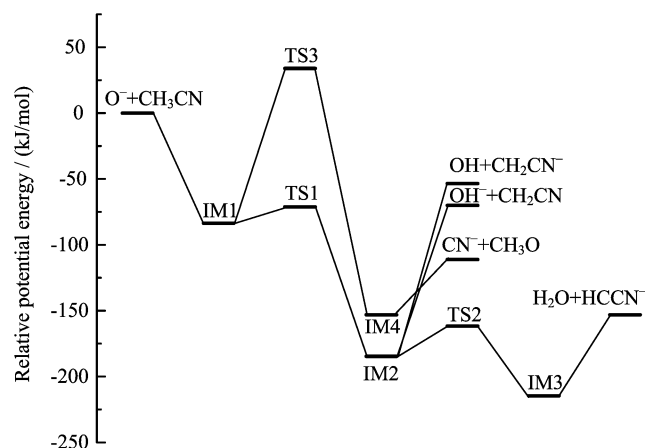


FIG. 2 Potential energy profile for the reaction of O<sup>-</sup> with CH<sub>3</sub>CN at our modified G3MP2B3 level of theory.

HCCN<sup>-</sup>. Thus, IM3 can directly dissociate to H<sub>2</sub>O and HCCN<sup>-</sup> at last. We have also tried to search the transition state corresponding to the reaction mechanism of H<sub>2</sub><sup>+</sup> concerted transfer, but no concerted transition state has been found, indicating that the H<sub>2</sub><sup>+</sup> transfer reaction channel observed in previous experiments should proceed via two-step isomerization indeed.

### C. S<sub>N</sub>2 reaction channel

As is known to all, potential energy profile for the S<sub>N</sub>2 reaction has two potential wells corresponding to

two ion-molecule complexes separated by a barrier [34]. As we have noted, only IM1 is located on the entrance-channel PES. IM1 can overcome TS3 to form IM4. Firstly, we try to optimize TS3 on the PES with the constraint of C<sub>3v</sub> symmetry for this S<sub>N</sub>2 channel, but the density matrix breaks the C<sub>3v</sub> symmetry. Thus, the optimized structure of TS3 is obtained finally with the C<sub>s</sub> symmetry. However, the molecular structure of TS3 is very near to C<sub>3v</sub> point group. Analysis of imaginary vibrational mode shows that TS3 is a typical S<sub>N</sub>2 reaction transition state. Reverse IRC calculation performed on TS3 leads to IM1 and forward IRC points to IM4. Both TS3 and IM4 are with <sup>2</sup>A' electronic ground states. Along the IRC, the charge transfers from O<sup>-</sup> anion to CN group, and IM4 is an ion-dipole complex formed by CN<sup>-</sup> and CH<sub>3</sub>O. Natural charge populated on CN group of IM4 is -0.706 while -0.294 on CH<sub>3</sub>O group, and the charge will continue to transfer from CH<sub>3</sub>O group to CN group when IM4 decomposes to CN<sup>-</sup> and CH<sub>3</sub>O.

### D. Comparison with experimental results

Figure 2 shows that the reaction pathway to H<sub>2</sub>O and HCCN<sup>-</sup> as products (corresponding to H<sub>2</sub><sup>+</sup> transfer) has the lowest rate-determining barrier. Therefore, under the thermal reaction condition around room temperature, the H<sub>2</sub><sup>+</sup> transfer channel is the most dominant among all the production channels. On the other hand, the S<sub>N</sub>2 reaction channel is hard to occur under the thermal reaction condition around room tempera-

ture, due to too large barrier height of TS3 relative to IM1. These conclusions are consistent with previous experimental conclusions [5, 7]. But with enough relative translational energy between  $O^-$  and  $CH_3CN$ , the  $S_N2$  reaction channel might occur with a certain probability.

As shown in Fig.2, the overall reaction processes of the  $H^+$  transfer and H-atom transfer channels are exothermic, and the dissociation limit of the former is slightly higher than that of the latter. Therefore, under the thermal reaction condition, the branching ratio of the  $H^+$  transfer channel should be slightly smaller than that of the H-atom transfer channel, and  $OH^-$  product should be measured with a larger branching ratio than  $CH_2CN^-$ . However, according to previous experimental results [5–7],  $CH_2CN^-$  from  $H^+$  transfer has been definitely observed with a larger branching ratio than  $OH^-$  from the H-atom transfer, which obviously disagrees with present calculations. A potential factor for this contradiction is due to the secondary reactions of initial anionic products. Grabowski and Melly have observed that both  $OH^-$  and  $HCCN^-$  react with  $CH_3CN$  via proton transfer to produce  $CH_2CN^-$  as secondary anionic product [7]. As a result, these two secondary reactions can decrease the branching ratios of  $OH^-$  and  $HCCN^-$ , and at the same time they increase the branching ratio of  $CH_2CN^-$ . We believe that these two secondary reactions are the key factors for the disagreement between our calculations and previous experiments. Thus the branching ratios for the title reaction should be further measured in experiment without influence of the secondary reactions, *e.g.* using crossed beam technique as Farrar *et al.* has done [16].

#### E. Comments on current hybrid functional B3LYP calculations

Hybrid functional B3LYP method has been utilized to characterize the stationary points on the PESs for the reactions of  $O^-$  with  $C_2H_4$  [13],  $C_2H_3$  [14],  $CH_3F$  [15],  $C_2H_2$  [16], and  $C_6H_6$  [17], however, our previous calculations show that the B3LYP method is not suitable to calculate accurate energies for the stationary points on the PES [13]. Therefore, high level G3B3 or G3MP2B3 methods [9] based on the B3LYP calculations should be employed to obtain more accurate energies for the stationary points on the PES, as present calculations have done.

As to the reaction of  $O^-$  with  $CH_3CN$ , a calculation problem is encountered while studying the  $H^+$  transfer and H-atom transfer channels. Based on the current B3LYP calculations, we cannot describe the  $OH^- \cdots CH_2CN$  and  $OH \cdots CH_2CN^-$  PESs separately, since we cannot control the charge to populate on OH group or  $CH_2CN$  group, neither can we locate the different transition states corresponding to  $H^+$  transfer and H-atom transfer channels respectively. Thus, the B3LYP method is not suitable to deal with the  $H^+$

transfer and H-atom transfer channels for the title reactive system. This limitation prevents us from performing further calculations of reaction kinetics and/or dynamics based on the present B3LYP reaction potential energy profile, *e.g.* RRKM calculations [35] and/or Born-Oppenheimer molecular dynamics (BOMD) simulations [36–39]. Recently, physical and chemical natures for the limitations of the current exchange-correlation functions have been elucidated by Cohen *et al.* [40]. Thus, the failure of the B3LYP method to model the  $H^+$  transfer and H-atom transfer reaction channels for the title reaction can be appointed to the delocalization error and static correlation error. Similarly, using other exchange-correlation functions should not successfully model the  $H^+$  transfer and H-atom transfer reaction channels for this reaction either, based on the same factors. In this case, the multi-configuration self-consistent-field (MCSCF) [41–43] method is expected to resolve this problem, but our primary calculations using MCSCF method to distinguish the  $H^+$  transfer and H-atom transfer reaction channels always fail due to convergence problems.

Fortunately, except for modeling the  $H^+$  transfer and H-atom transfer channels on the exit-channel PES of the title reaction, the other B3LYP calculations including geometry optimizations and frequency calculations are believed to be reliable.

#### IV. CONCLUSION

The potential energy profile and reaction mechanism for the reaction of  $O^-$  with  $CH_3CN$  have been studied with the high level G3MP2B3 method. Four possible production channels are examined respectively, as  $H^+$  transfer, H-atom transfer,  $H_2^+$  transfer, and  $S_N2$  reaction pathways. Based on our calculations, at thermal reaction condition around room temperature, the  $H_2^+$  transfer channel is the most dominant production pathway, and the  $S_N2$  channel is difficult to occur, which agrees with previous experimental conclusions.

However, our detailed calculations show that the B3LYP method can not describe the  $H^+$  transfer and H-atom transfer channels fully and properly. Fortunately, besides modeling the  $H^+$  transfer and H-atom transfer channels on the exit-channel PES of this reaction, the other B3LYP calculations including geometry optimizations and frequency calculations are still reliable.

#### V. ACKNOWLEDGMENTS

This work is supported by the National Natural Science Foundation of China (No.20603033 and No.10979042) and the National Key Basic Research Special Foundation (No.2007CB815204).

- [1] J. Lee and J. J. Grabowski, *Chem. Rev.* **92**, 1611 (1992), and references therein.
- [2] M. Born, S. Ingemann, and N. M. M. Nibbering, *Mass Spectrom. Rev.* **16**, 181 (1997).
- [3] M. J. Jensen, U. V. Pedersen, and L. H. Andersen, *Phys. Rev. Lett.* **84**, 1128 (2000).
- [4] M. Born, S. Ingemann, and N. M. M. Nibbering, *J. Am. Chem. Soc.* **116**, 7210 (1994).
- [5] J. H. J. Dawson and K. R. Jennings, *J. Chem. Soc. Faraday Trans. 2* **72**, 700 (1976).
- [6] W. Lindinger, T. D. Märk, and F. Howorka, *Swarms of Ions and Electrons in Gases*, New York: Springer-Verlag, 226 (1984).
- [7] J. J. Grabowski and S. J. Melly, *Int. J. Mass Spectrom. Ion Processes* **81**, 147 (1987).
- [8] X. Yang, X. Zhang, and A. W. Castleman Jr., *J. Phys. Chem.* **95**, 8520 (1991).
- [9] A. G. Baboul, L. A. Curtiss, P. C. Redfern, and K. Raghavachari, *J. Chem. Phys.* **110**, 7650 (1999).
- [10] C. Lee, W. Yang, and R. G. Parr, *Phys. Rev. B* **37**, 785 (1988).
- [11] A. D. Becke, *J. Chem. Phys.* **98**, 5648 (1993).
- [12] M. J. Frisch, G. W. Trucks, H. B. Schlegel, G. E. Scuseria, M. A. Robb, J. R. Cheeseman, J. A. Montgomery, Jr., T. Vreven, K. N. Kudin, J. C. Burant, J. M. Millam, S. S. Iyengar, J. Tomasi, V. Barone, B. Mennucci, M. Cossi, G. Scalmani, N. Rega, G. A. Petersson, H. Nakatsuji, M. Hada, M. Ehara, K. Toyota, R. Fukuda, J. Hasegawa, M. Ishida, T. Nakajima, Y. Honda, O. Kitao, H. Nakai, M. Klene, X. Li, J. E. Knox, H. P. Hratchian, J. B. Cross, C. Adamo, J. Jaramillo, R. Gomperts, R. E. Stratmann, O. Yazyev, A. J. Austin, R. Cammi, C. Pomelli, J. W. Ochterski, P. Y. Ayala, K. Morokuma, G. A. Voth, P. Salvador, J. J. Dannenberg, V. G. Zakrzewski, S. Dapprich, A. D. Daniels, M. C. Strain, O. Farkas, D. K. Malick, A. D. Rabuck, K. Raghavachari, J. B. Foresman, J. V. Ortiz, Q. Cui, A. G. Baboul, S. Clifford, J. Cioslowski, B. B. Stefanov, G. Liu, A. Liashenko, P. Piskorz, I. Komaromi, R. L. Martin, D. J. Fox, T. Keith, M. A. Al-Laham, C. Y. Peng, A. Nanayakkara, M. Challacombe, P. M. W. Gill, B. Johnson, W. Chen, M. W. Wong, C. Gonzalez, and J. A. Pople, *Gaussian 03, Revision B.05*, Pittsburgh PA: Gaussian, Inc. (2003).
- [13] F. Yu, Y. G. Zhao, Y. Wang, X. G. Zhou, and S. L. Liu, *Acta Chim. Sin.* **65**, 899 (2007).
- [14] X. L. Wang, F. Yu, D. Xie, S. L. Liu, and X. G. Zhou, *Acta Chim. Sin.* **66**, 2499 (2008).
- [15] M. Yamamoto, K. Yamashita, and M. Sadakata, *J. Mol. Struct.: THEOCHEM* **634**, 31 (2003).
- [16] L. Liu, Y. Li, and J. M. Farrar, *J. Chem. Phys.* **123**, 94304 (2005).
- [17] Y. G. Zhao, X. G. Zhou, F. Yu, J. H. Dai, and S. L. Liu, *Acta Phys. Chim. Sin.* **22**, 1095 (2006).
- [18] M. J. Frisch, J. A. Pople, and J. S. Binkley, *J. Chem. Phys.* **80**, 3265 (1984).
- [19] J. Simons and K. D. Jordan, *Chem. Rev.* **87**, 535 (1987).
- [20] A. P. Scott and L. Radom, *J. Phys. Chem.* **100**, 16502 (1996).
- [21] C. Gonzalez and H. B. Schlegel, *J. Chem. Phys.* **90**, 2154 (1989).
- [22] C. Gonzalez and H. B. Schlegel, *J. Phys. Chem.* **94**, 5523 (1990).
- [23] E. D. Glendening, A. E. Reed, J. E. Carpenter, and F. Weinhold, NBO Version 3.1.
- [24] A. E. Reed and F. Weinhold, *J. Chem. Phys.* **78**, 4066 (1983).
- [25] A. E. Reed, R. B. Weinstock, and F. Weinhold, *J. Chem. Phys.* **83**, 735 (1985).
- [26] J. E. Carpenter and F. Weinhold, *J. Mol. Struct.: THEOCHEM* **169**, 41 (1988).
- [27] A. E. Reed, L. A. Curtiss, and F. Weinhold, *Chem. Rev.* **88**, 899 (1988).
- [28] H. B. Schlegel, *J. Chem. Phys.* **84**, 4530 (1986).
- [29] C. Sosa and H. B. Schlegel, *Int. J. Quantum Chem.* **29**, 1001 (1986).
- [30] C. Sosa and H. B. Schlegel, *Int. J. Quantum Chem.* **30**, 155 (1986).
- [31] R. A. Kendall, T. H. Dunning Jr., and R. J. Harrison, *J. Chem. Phys.* **96**, 6796 (1992).
- [32] E. P. F. Lee and J. M. Dyke, *Mol. Phys.* **88**, 143 (1996).
- [33] M. Yamamoto, K. Yamashita, and M. Sadakata, *Bull. Chem. Soc. Jpn.* **75**, 1483 (2002).
- [34] W. N. Olmstead and J. I. Brauman, *J. Am. Chem. Soc.* **99**, 4219 (1977).
- [35] K. A. Holbrook, M. J. Pilling, and S. H. Robertson, *Unimolecular Reactions*, 2nd Edn., New York: John Wiley & Sons, 39 (1996).
- [36] H. B. Schlegel, *J. Comput. Chem.* **24**, 1514 (2003).
- [37] W. Chen, W. L. Hase, and H. B. Schlegel, *Chem. Phys. Lett.* **228**, 436 (1994).
- [38] J. M. Millam, V. Bakken, W. Chen, W. L. Hase, and H. B. Schlegel, *J. Chem. Phys.* **111**, 3800 (1999).
- [39] X. Li, J. M. Millam, and H. B. Schlegel, *J. Chem. Phys.* **113**, 10062 (2000).
- [40] A. J. Cohen, P. Mori-Sánchez, and W. Yang, *Science* **321**, 792 (2008).
- [41] H. B. Schlegel and M. A. Robb, *Chem. Phys. Lett.* **93**, 43 (1982).
- [42] N. Yamamoto, T. Vreven, M. A. Robb, M. J. Frisch, and H. B. Schlegel, *Chem. Phys. Lett.* **250**, 373 (1996).
- [43] M. J. Frisch, I. N. Ragazos, M. A. Robb, and H. B. Schlegel, *Chem. Phys. Lett.* **189**, 524 (1992).